molecular pharmaceutics

ARTICLE

pubs.acs.org/molecularpharmaceutics

Duplex End Breathing Determines Serum Stability and Intracellular Potency of siRNA−Au NPs

Pinal C. Patel,[†,‡] Liangliang Hao,[†,‡] Weng Si Au Yeung,[†,‡] and Chad A. Mirkin*[,‡,§]

[†]Interdepartmental Biological Sciences Program, [§]Department of Chemistry, and [‡]International Institute for Nanotechnology, Northwestern University, 2145 Sheridan Road, Evanston, Illinois 60208-3113, United States

ABSTRACT: Structural requirements of siRNA-functionalized gold nanoparticles (siRNA−Au NPs) for Dicer recognition and serum stability were studied. We show that the 3′ overhang on the nucleic acids of these particles is preferentially recognized by Dicer but also makes the siRNA duplexes more susceptible to nonspecific serum degradation. Dicer and serum nucleases show lower preference for blunt duplexes as opposed to those with 3′ overhangs. Importantly, gold nanoparticles functionalized with blunt duplexes with relatively less thermal breathing are up to 15 times more stable against serum degradation without compromising Dicer recognition. This increased stability leads to a 300% increase in cellular uptake of siRNA−Au NPs and improved gene knockdown.

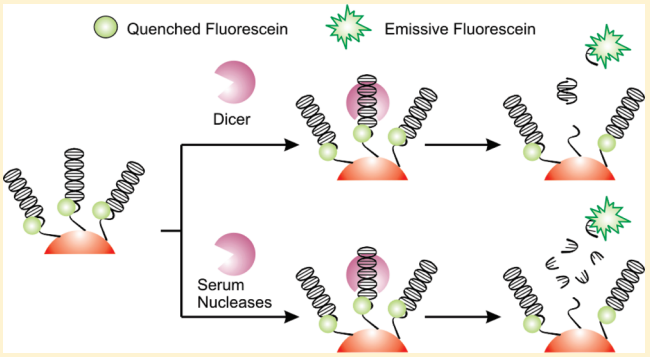

KEYWORDS: siRNA, gold nanoparticle, siRNA stability, GFP knockdown, Dicer activity

INTRODUCTION

RNA interference (RNAi) is a potent gene regulatory mechanism that leads to the inhibition of target genes in a sequence dependent manner.[1] This process is triggered by double stranded RNAs, known as small interfering RNAs (siRNAs),[2] that are recognized by the RNA-induced Silencing Complex (RISC). Dicer, an endoribonuclease, binds and cleaves long dsRNA[3] to generate siRNA, 18−22bp in length. RISC then binds to the siRNA leading to passenger strand cleavage.[4] The complementary strand, known as the guide strand, is used by the active RISC to find the target sequence along the mRNA by complementary base interactions. Finally, RISC acts as an endonuclease to cleave the target mRNA, preventing its translation into the corresponding protein. This mechanism of selectively controlling protein expression has sparked interest in harnessing RNAi for disease management and treatment by delivering siRNAs targeting specific proteins of interest to cells.

However, the delivery of small RNAs to cells must overcome several challenges to be effective as a therapeutic. The RNA must be stable against extracellular nucleases which nonspecifically degrade small RNA sequences.[5−7] It must be able to enter the cells without the aid of toxic agents or untenable techniques, such as electroporation[5] and microinjection.[8] Finally, it must be able to participate in the natural pathway of RNAi. Unmodified siRNAs degrade within several minutes while in blood and serum.[9,10] Numerous modifications to the phosphate backbone and the 2′ position of the sugar have been used to stabilize RNA against nonspecific nucleases.[11,12] However, these modifications can have negative side effects, such as nonspecific protein binding and increased toxicity,[13] decrease participation in the RNAi pathway and intracellular activity,[14] and have unknown long-term effects. Cellular delivery of siRNA has been realized with complexation/conjugation with auxiliary chemical reagents[15−17] or via electroporation.[18] However, these techniques lead to undesired toxicity and are difficult to translate to more complex animal model organisms and clinical settings.[17] Nonetheless, recent reports using lipid complexation have shown improved stability[19] resulting in *in vivo* applications in animals[20,21] and humans.[22]

Nanomaterials are becoming promising constructs for drug delivery, disease detection, molecular diagnostics and intracellular gene regulation.[23−35] In 1996, we introduced the concept of the polyvalent nucleic acid nanoparticle conjugate,[36] and subsequently identified several unique properties associated with it[37−40] and developed it for many *in vitro* molecular diagnostic[41−43] and intracellular gene regulation applications.[44] In 2009, we devised a procedure for synthesizing polyvalent siRNA functionalized gold nanoparticles (siRNA−Au NPs) and explored their utility for intracellular gene regulation.[45] Through these studies, we have discovered that these hybrid nanomaterials have unique composite properties that make them attractive for biological applications.[46] They have been shown to enter cultured cells (over 50 different cell lines) without the need to use transfection agents, such as cationic lipids. They stabilize the conjugated siRNAs against degradation by serum nucleases without any chemical modifications of the siRNA.[45] They exhibit significantly less induction of innate immune response compared to their molecular counterparts.[37] While nucleic acids and siRNAs, in particular, have been conjugated

Received: February 22, 2011
Accepted: June 1, 2011
Revised: April 26, 2011
Published: June 01, 2011

to gold nanoparticles[47,48] or quantum dots,[18,49] detailed studies of the structural features that impart nuclease stability and Dicer recognition on nanoparticles have not been conducted. We have conducted such a study that allows us to determine the features of siRNA−Au NPs that are critical to their stability in serum and recognition by Dicer.

EXPERIMENTAL SECTION

Synthesis of Gold Nanoparticles and RNA. Citrate stabilized gold nanoparticles (13 ± 1 nm) were prepared using the Frens method[50] and rendered RNase-free by treatment with 0.1% diethylpyrocarbonate (DEPC, Sigma) followed by autoclaving to inactivate DEPC. RNA oligonucleotides were synthesized using TOM-RNA reagents (Glen Research) on a MerMade 6 system (Bioautomation) using manufacturer recommended cleavage and deprotection protocols. All oligonucleotides were purified using reverse-phase high performance liquid chromatography (RP-HPLC) on a Varian Microsorb C_{18} column (10 μm, 300 × 10 mm) with 0.1 M triethylammonium acetate (TEAA), pH 7 using a 1%/min gradient of 100% CH_3CN at a flow rate of 3 mL/min, while monitoring the UV signal of the nucleic acids at 254 nm. The aqueous buffer was DEPC treated (0.1% v/v) and autoclaved before use. After purification, the oligonucleotides were lyophilized and stored at −80 °C until use. The following sequences that target enhanced green fluorescent protein (eGFP) mRNA were made (all listed 5′ to 3′): phosphate - ACC CUG AAG UUC AUC UGC ACC ACC G (hexaethyleneglycol)$_2$ − propyl thiol, CGG UGG UGC AGA UGA ACU UCA GGG UCA, fluorescein - CGG UGG UGC AGA UGA ACU UCA GGG UCA, CGG UGG UGC AGA UGA ACU UCA GGG U, fluorescein - CGG UGG UGC AGA UGA ACU UCA GGG U, CGG UGG UGC AGA UGA ACU UCA GGG U**CA**, fluorescein - CGG UGG UGC AGA UGA ACU UCA GGG U**CA**, CGG UGG UGC AGA UGA ACU UCA GGG U*C*A, fluorescein - CGG UGG UGC AGA UGA ACU UCA GGG U*C*A, CGG UGG UGC AGA UGA ACU UCA GGG U***C*A**, fluorescein - CGG UGG UGC AGA UGA ACU UCA GGG U***C*A**, phosphate - CGG UGG UGC AGA UGA ACU UCA GGG U (hexaethyleneglycol)$_2$ − propyl thiol, ACC CUG AAG UUC AUC UGC ACC ACC G, fluorescein - ACC CUG AAG UUC AUC UGC ACC ACC G. Bold letters indicate locked nucleic acid (Exiqon) residues, and * indicates phosphorothioate substitution.

Synthesis of siRNA−Au NPs and RNA Loading Measurements. Gold nanoparticles were functionalized with siRNA duplexes as described previously.[45] To measure the surface coverage of RNA on nanoparticles, the concentration of fluorescein-labeled siRNA functionalized nanoparticles was determined by measuring the intensity of the surface plasmon resonance band at 524 nm by UV−vis spectroscopy and using the Beer−Lambert law. The nanoparticles were then dissolved with potassium cyanide (5 mM final), and the fluorescence of the sample was measured on a FluoDia T70 plate reader (Photon Technology International). This fluorescence was compared to a standard curve generated using the same fluorescein-labeled RNA sequence. The measured concentration of RNA was divided by the measured concentration of nanoparticle to derive the average RNA loading per nanoparticle.

Dicer Activity and Nuclease Assays. Dicer activity assays were performed using published protocols in a semiclear 96-well, PCR plate using a FluoDia T70 plate reader (Photon Technology International).[40] Briefly, fluorescein containing siRNA−Au NPs (5 nM final) were mixed with reaction buffer[51] (20% glycerol, 60 mM Tris-HCl, 10 mM $MgCl_2$ and 0.5 mM DTT, 1 mM ATP) and allowed to equilibrate at 37 °C. Recombinant human Dicer (Invitrogen) was added to the assay well, followed by 40 μL of mineral oil (Bio-Rad) layered on top to prevent evaporation. Degradation of the RNA by Dicer was monitored by measuring an increase in the fluorescence signal as the fluorescein (excitation = 480 nm, emission = 530 nm) was dissociated from the gold nanoparticles. Stability of siRNA−Au NPs against serum degradation was measured under identical assay conditions with heat inactivated fetal bovine serum (FBS, 10% final, Mediatech) substituted for Dicer. The reactions with Dicer and 10% FBS were monitored for four hours at 30 s intervals, and the activity rates were determined by calculating the slope of the fluorescence curve from the first 30 points. All substrates were tested at least three times in each assay to ascertain variability. The amount of substrate catalyzed was calculated by first determining the fluorescence signal generated from complete dehybridization of the fluorescein-labeled RNA from a 5 nM solution of Au NPs and setting this level of fluorescence to the maximum level of fluorescence possible for a 5 nM solution of the substrate (fluorescein modified siRNA−Au NPs). Fluorescence level in buffer alone was assigned the value of 0 nM substrate catalyzed. These two values were used to construct a linear plot for comparison with the unknowns.

Measuring Knockdown by Real Time Polymerase Chain Reaction and eGFP Fluorescence. Mouse endothelial cells stably expressing eGFP (C166-eGFP) were purchased from ATCC and cultured as recommended. For a typical experiment, cells were grown in a tissue culture treated plate (Corning) at 5000 cells/well and various siRNA−Au NPs were added to the cells in serum containing media at a solution concentration of 10 nM. After three days of incubation, the cells were washed twice with phosphate buffered saline (Hyclone), trypsinized and counted using the Viacount reagent (Millipore) on a Guava Easycyte Mini. The cells were processed with the Cell-to-cDNA kit (Ambion), and the relative levels of eGFP mRNA were quantified using the SYBR Green rt-PCR mix (Roche) on a Lightcycler 2.0 system (Roche). ApoB was used as an internal control. The expression levels of eGFP and percentage knockdown were calculated using comparative Ct method. Primers used for rt-PCR were GFP forward (5′ CCA CAT GAA GCA GCA CGA CTT 3′), GFP reverse (5′ GGT GCG CTC CTG GAC GTA 3′), ApoB forward (5′ CAC GTG GGC TCC AGC ATT 3′) and ApoB reverse (5′ TCA CCA GTC ATT TCT GCC TTT G 3′). All primers were purchased from Integrated DNA Technologies. Knockdown of eGFP protein was measured by fluorescence quantification at room temperature using a published protocol.[44] Statistical analyses between individual groups were performed by a Student t test; a P value of <0.05 was considered statistically significant.

Cellular Uptake Studies. The average number of gold nanoparticles per cell for each siRNA−Au NP substrate was determined using inductively coupled plasma mass spectrometry (ICP-MS, Thermo-Fisher) following published protocols.[52] Briefly, C166-GFP cells were cultured in the presence of a 10 nM solution concentration of siRNA−Au NPs. After 72 h, the cells were washed with PBS, trypsinized and counted. The cells were centrifuged (750 rcf, 10 min) to remove the media, resuspended in a solution of 3% hydrochloric acid in nitric acid, and incubated at 60 °C overnight to digest the samples. The digests were diluted in a matrix consisting of 2% HNO_3, 2% HCl and 1 ppb Indium

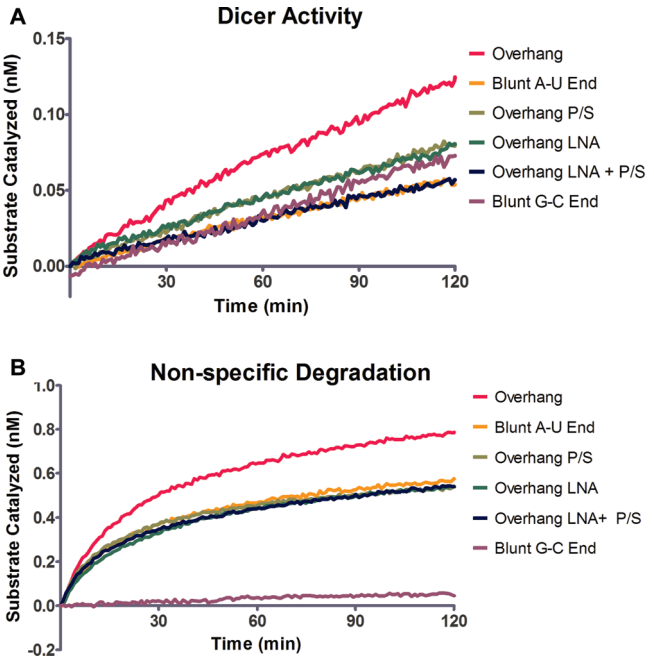

Figure 1. Analysis of siRNA−Au NPs in enzymatic assays with Dicer (A) and 10% FBS (B). In panel A, recombinant Dicer shows a preference for the siRNA−Au NP substrates with a 3′ overhang. Substrates with modifications on the 3′ overhang (phosphorothioate, LNA or both) or no overhang show lower Dicer activity. In panel B, nonspecific degradation in 10% FBS is higher for siRNA−Au NPs containing single-stranded overhangs. Modifications to the overhang region decrease the nonspecific degradation slightly. Highest stability against nonspecific degradation is imparted by blunt duplexes with distal, thermally stable ends.

(internal standard). The gold content of the cell digests was determined by comparison with a standard curve (0 to 200 ppb Au) made from a gold standard (Sigma) prepared in the same matrix. The number of nanoparticles in each sample was calculated based on the concentration of Au found in the sample.

RESULTS

Dicer and Serum Nucleases Show Preference for the 3′ 2-Base Overhang of the Antisense Strand. To investigate the structural basis of serum stability and Dicer activation on nanoparticles, we examined anti-eGFP Dicer substrate RNAs of 25−27 base pairs[53,54] immobilized on 13 nm gold nanoparticles using a fluorescence recovery assay.[40] Gold nanoparticles were functionalized with fluorescein-labeled siRNA (siRNA−Au NPs) following published procedures,[45] and RNA loading per nanoparticle was measured. All samples were found to have 50 ± 4 duplexes per nanoparticle. To measure Dicer activity or serum stability, recombinant human Dicer (1 unit) or FBS (10% final) was added to a solution containing 5 nM siRNA−Au NP substrates in the reaction at 37 °C, and the fluorescence increase was monitored (Figure 1). Initially, we tested two siRNA−Au NP substrates, one with a 2-bp overhang on the 3′ terminus of the antisense strand (termed overhang substrate) to mimic the widely used molecular siRNAs and one with a blunt end (termed blunt A-U substrate) (Scheme 1). The overhang contains C and A in the penultimate and terminal positions to maximize Dicer recognition.[55] The sense strand with a 5′ phosphate group, an

Scheme 1. (A) Sequences and Arrangement of siRNA Substrate on the Nanoparticles Used in This Study[a]. (B) Scheme of a Typical Dicer or Serum Nuclease Activity Assay[b]

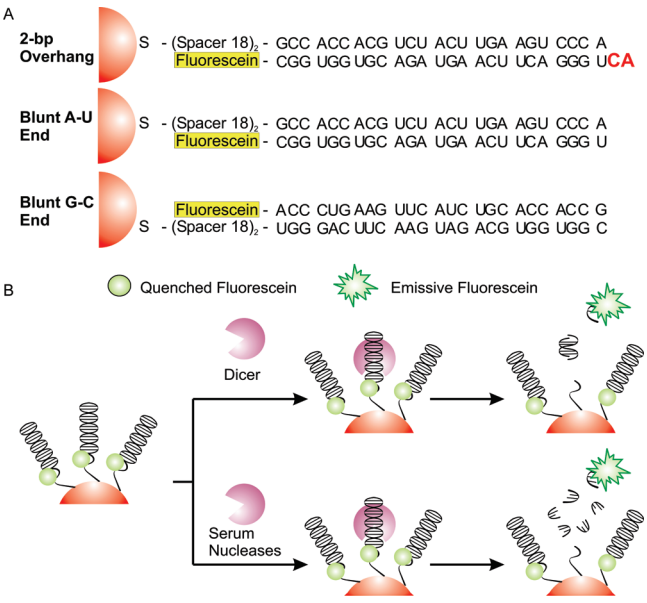

[a] In some experiments, the 2-bp overhang (in red) was modified by addition of phosphorothioate linkages, LNA phosphoramidites or both and is indicated as overhang P/S, overhang LNA or overhang LNA + P/S, respectively. In all cases, the sense strand is shown on top. [b] Gold nanoparticles functionalized with fluorophore-labeled siRNAs are incubated in the presence of nucleases at 37 °C. The change in fluorescence is measured over time to assess the activity of the nucleases (see Experimental Section).

ethylene glycol spacer, and a 3′ propylthiol modification was used to attach the duplexes to gold nanoparticles.

The results of these experiments demonstrate that Dicer has a preference for siRNA duplexes with 3′ overhangs on the RNA−Au NP (Figure 1). The catalysis rate was approximately twice as fast for the overhang substrates compared with blunt A-U substrates (1.23×10^{-3} nM/min and 5.71×10^{-4} nM/min for overhang and blunt A-U substrates respectively, Table 1). These results confirm the studies from the molecular system[55,56] on this enzyme. Interestingly, the overhang substrates were also approximately 40% more susceptible to nonspecific degradation in serum compared to the blunt A-U substrates (1.16×10^{-2} nM/min vs 8.43×10^{-3} nM/min for overhang vs blunt substrates). Importantly, for siRNA−Au NPs, the nonspecific activity from general nucleases was 10−15-fold higher than the specific activity from Dicer (Table 1). These results show that the 2-base overhang is responsible for increasing the Dicer recognition of siRNA−Au NPs. However, the same structural feature also makes the siRNA−Au NPs more susceptible to nonspecific degradation, presumably due to activity of RNase A family or similar processive exonuclease.[57]

Chemical Modifications to the Overhang Region Lower Dicer Processing and Serum Degradation. Serum stability is a desirable trait of any siRNA conjugate. Since the 2-base overhang made siRNA−Au NPs more susceptible to nonspecific degradation, we hypothesized that, by modifying the overhang positions in an attempt to stabilize them, we can increase the serum stability of siRNA−Au NP substrates. While specialty oligonucleotides are

Table 1. The Rates of Catalysis of Double-Stranded RNA by Dicer and 10% FBS at 37 °C[a]

	Catalytic Activity (nM substrate catalyzed/min)				
	Dicer		FBS		
	rate	std dev	rate	std dev	FBS/Dicer
overhang	1.23×10^{-3}	1.06×10^{-4}	1.16×10^{-2}	4.36×10^{-4}	9.43
Blunt A-U	5.71×10^{-4}	3.79×10^{-5}	8.43×10^{-3}	1.94×10^{-4}	14.77
overhang P/S	7.68×10^{-4}	8.66×10^{-5}	7.82×10^{-3}	3.64×10^{-4}	10.18
overhang LNA	6.82×10^{-4}	2.91×10^{-5}	7.80×10^{-3}	1.58×10^{-4}	11.44
overhang LNA + P/S	4.61×10^{-4}	3.81×10^{-5}	7.37×10^{-3}	2.82×10^{-4}	15.99
Blunt G-C	6.24×10^{-4}	1.98×10^{-4}	4.99×10^{-4}	7.12×10^{-5}	0.80

[a] The rates were determined by taking the slope of the activity curves over the first 15 min of the fluorescence recovery assay described in the Experimental Section.

available and used by researchers,[9,11,12,19,58−65] we chose locked nucleic acids (LNA) and structures with phosphorothioates as representative modifications of the pentose sugar and phosphate backbone respectively. The use of LNA bases or phosphorothioate modification has been shown to increase stability of RNA to nonspecific degradation.[61,66] Researchers have suggested that some modifications, such as phosphorothioate, improve nuclease resistance of siRNA by promoting secondary structures that affect recognition or binding by nucleases.[67] Additionally, modest LNA and phosphorothioate substitutions have been shown to be compatible with RNAi.[14,58,64,68] When we modified the 2-base overhang region by changing the terminal two bases of the antisense strand to LNA, inserting phosphorothioate linkages at the 3′ terminus or both, the stability of these substrates against nonspecific degradation increased modestly (Figure 1, Table 1), from 1.16×10^{-2} nM/min for the unmodified substrate to 7.37×10^{-3} nM/min for substrates containing both LNA and phosphorothioate modifications in the overhang, a 40% increase in serum stability. However, their ability to be processed by Dicer decreased by 60% (1.23×10^{-3} nM/min for the unmodified substrate vs 4.61×10^{-4} nM/min substrates containing both LNA and phosphorothioate modifications), indicating that modifications to the antisense strand can affect Dicer recognition and processing. Interestingly, the nonspecific nuclease activity remained 10−15-fold higher than Dicer activity, meaning that we were trading stability for specificity. These experiments show that modifying the overhang positions had similar effects on the ability of nonspecific nucleases and Dicer to recognize and process siRNA−Au NPs.

Serum Stability Is Increased by Thermal Stability of the Distal End of siRNA Duplex. We have previously reported that high oligonucleotide density and high local salt concentration near the nanoparticle surface[40] impart serum stability to oligonucleotides. However, for siRNA−Au NPs, we sought to improve the serum stability while keeping the relative Dicer specificity high. It is known that single-stranded RNA is less stable than double stranded RNA[12,65] and that single stranded regions of RNA are potential substrates for processive enzymes of RNase A family of exonucleases.[57,69] In the blunt A-U substrates, the duplex breathing at the solution end could generate single-stranded regions that play a role in the susceptibility of siRNAs to nuclease degradation. For the blunt duplex that we studied, the binding energies (37 °C and 10 mM Mg^{2+}) of the last five bases of the two ends were computationally predicted by mfold[70] to be $\Delta G = -7.4$ kcal/mol (G-C end) and −6.1 kcal/mol (A-U end) and the T_ms of the same regions were estimated to be 12.1 °C and <10 °C respectively. We hypothesized that if we reversed the orientation of the duplex on the nanoparticle so that the more stable end was distal to the nanoparticles and therefore interacted with proteins, the serum stability might improve. Indeed, when we changed the orientation of the siRNA on nanoparticles so that the end with a G-C base pair (termed blunt G-C) was presented to the solution and thus enzymes, the serum degradation rate decreased to 4.99×10^{-4} nM/min compared with 7.37×10^{-3} nM/min for blunt A-U substrates, a 93% decrease in serum degradation (Figure 1). This same substrate was still recognized by Dicer (6.24×10^{-4} nM/min) to an extent similar to the blunt A-U substrate. Importantly, the nonspecific nuclease activity was now 25% lower than Dicer activity, compared to 10−15-fold higher in previous substrates (Table 1), suggesting that we had "turned down" the nonspecific nucleases without substantially affecting Dicer activity.

The results of these experiments show that, in polyvalent siRNA−Au NPs, the stability of the part of the duplex that is oriented away from nanoparticle surface and into the solution plays a key role in its nuclease resistance. In the context of siRNA−Au NPs, the distal or solution end of duplex is more critical for protein binding because the proximal end is essentially inaccessible to proteins due to steric hindrance resulting from nanoparticle functionalization. Of the two blunt siRNA−Au NP conjugates, the conjugates with the more stable distal ends showed 15-fold higher resistance to serum nucleases. The same duplexes, when free in solution, were degraded equally rapidly by 10% FBS (>80% degraded within 15 min, data not shown). Importantly, this arrangement maintains Dicer recognition and processing. While we have previously observed that the nanoparticle functionalization can increase the nuclease resistance of oligonucleotides compared to free oligonucleotides,[40,45] this is the first study that shows that strand orientation on nanoparticles, and in particular end breathing, has significant consequences on Dicer recognition and selective nuclease degradation.

Increased Stability in Serum Results in Higher Intracellular Activity. Having designed and prepared a number of siRNA−Au NP substrates with different serum degradation rates, we next studied their ability to knockdown eGFP in cell cultures. C166-GFP cells were treated with the three types of siRNA−Au NPs targeting eGFP mRNA, and control nanoparticles functionalized with nonspecific RNA sequence, respectively, in culture media containing 10% FBS at 37 °C. Three days following the nanoparticle treatment, the cells were analyzed for eGFP mRNA

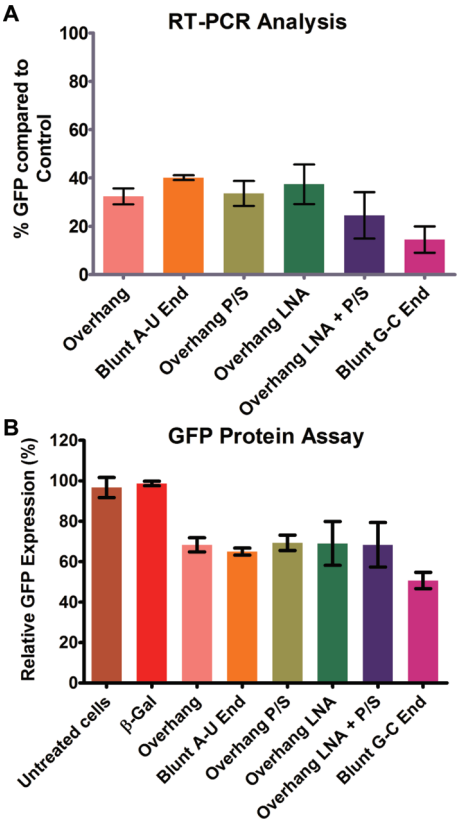

Figure 2. Quantification of eGFP knockdown in mouse endothelial cells using real-time polymerase chain reaction (rt-PCR) (A) and fluorescent protein assay (B). In both assays, the siRNA—Au NPs that were most stable against serum degradation showed the highest knockdown. The results are average of three independent experiments. In both assays, the results from blunt G-C substrates were found to be statistically significant ($p < 0.05$) in Student's t test compared with all the other GFP siRNAs tested.

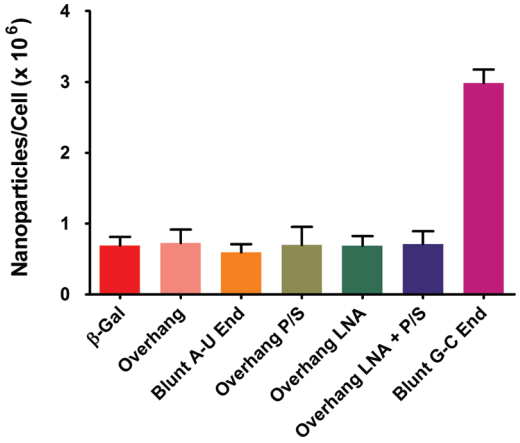

Figure 3. Cellular uptake of siRNA—Au NPs in C166-GFP cells. The data show that the siRNA—Au NPs with highest stability against serum degradation exhibited highest cellular uptake. The high uptake correlates with higher knockdown of target protein.

using real time polymerase chain reaction (rt-PCR) and for eGFP protein using fluorescence protein assays.[44] They were compared with cells that had not been treated with nanoparticles. We hypothesized that if the siRNA—Au NPs are more stable during the course of the experiment, then improved knockdown may be observed. Indeed, the results of the rt-PCR analyses indicate that the siRNA—Au NPs with the highest stability against serum degradation also showed the highest eGFP knockdown (Figure 2A,B). For example, cellular treatment with the nanoparticles functionalized with the overhang substrates resulted in GFP knockdown of 65.6 ± 4.0%, whereas the treatment with nanoparticles functionalized with blunt G-C siRNA resulted in GFP knockdown of 85.5 ± 4.8% as determined by rt-PCR. The results of the protein assay confirmed these findings.

Additionally, when we measured the cellular uptake of these siRNA—Au NPs, the conjugates with highest stability were also internalized to the greatest extent (Figure 3). For example, the siRNA—Au NPs containing overhang substrates, modified overhang substrates, or blunt A-U substrates had cellular uptake of $6.90 \times 10^5 \pm 1.2 \times 10^5$, $7.2 \times 10^5 \pm 1.8 \times 10^5$, and $6.98 \times 10^5 \pm 1.1 \times 10^5$ nanoparticles/cell, respectively. However, the siRNA—Au NPs functionalized with blunt G-C substrates contained $2.98 \times 10^6 \pm 1.90 \times 10^5$ nanoparticles/cell, a 300% increase. Significant changes in uptake were not observed for the siRNA—Au NPs containing overhang substrates, modified overhang substrates, or blunt A-U substrates, because the difference in their serum stabilities is relatively small (<2-fold). The nanoparticle conjugates that showed the highest uptake were 15—20 times more stable compared to the other particles, as determined by serum nuclease activity rate. These results are consistent with our previous observation that increasing the density of oligonucleotides on gold nanoparticles increases their cellular uptake.[52] In the case of siRNA—Au NPs, as serum nucleases degrade the siRNA, fewer oligonucleotides remain on the particles, resulting in structures that are less likely to be internalized by cells. However, when the siRNA is stabilized on the nanoparticles, the polyvalent structure remains intact over the course of the experiment. This increases the likelihood of binding with cellular proteins, such as scavenger receptors, that mediate cellular uptake[71] thus leading to higher degrees of cellular internalization. The resulting increase in the intracellular concentration of active siRNA—Au NPs results in higher levels of gene knockdown.

SUMMARY

In summary, we have shown that Dicer processing and serum stability of siRNA—Au NPs can vary dramatically with minor changes in nucleic acid structural features, such as distal 3′ overhangs. The serum stability can be increased by as much as 15-fold for siRNA structures with blunt ends of high thermal stability and low duplex breathing. This structural change leads to a modest 2-fold decrease in Dicer recognition and processing. However, the increased serum stability enhances cellular uptake by 300% and thus leads to greater gene knockdown. The observations reported in this article will allow researchers working with nanoparticle (and polyvalent nucleic acid) based siRNA delivery methods to improve their substrate design and cellular effects.

AUTHOR INFORMATION

Corresponding Author

*Northwestern University, Department of Chemistry, 2145 Sheridan Road, Evanston Campus 3113, Evanston, Illinois 60208-3113. Tel: (847) 491-2907. Fax: (847) 467-5123 . E-mail: chadnano@northwestern.edu.

■ ACKNOWLEDGMENT

C.A.M. acknowledges a Cancer Center for Nanotechnology Excellence (NCI-CCNE) award and the AFOSR for support of this research. P.C.P. was supported by a Ryan Fellowship.

■ REFERENCES

(1) Fire, A.; Xu, S. Q.; Montgomery, M. K.; Kostas, S. A.; Driver, S. E.; Mello, C. C. Potent and specific genetic interference by double-stranded RNA in *Caenorhabditis elegans*. *Nature* **1998**, *391* (6669), 806–811.

(2) Elbashir, S. M.; Harborth, J.; Lendeckel, W.; Yalcin, A.; Weber, K.; Tuschl, T. Duplexes of 21-nucleotide RNAs mediate RNA interference in cultured mammalian cells. *Nature* **2001**, *411* (6836), 494–498.

(3) Jinek, M.; Doudna, J. A. A three-dimensional view of the molecular machinery of RNA interference. *Nature* **2009**, *457* (7228), 405–412.

(4) Matranga, C.; Tomari, Y.; Shin, C.; Bartel, D. P.; Zamore, P. D. Passenger-strand cleavage facilitates assembly of siRNA into Ago2-containing RNAi enzyme complexes. *Cell* **2005**, *123* (4), 607–620.

(5) Bartlett, D. W.; Davis, M. E. Effect of siRNA nuclease stability on the *in vitro* and *in vivo* kinetics of siRNA-mediated gene silencing. *Biotechnol. Bioeng.* **2007**, *97* (4), 909–921.

(6) Hickerson, R. P.; Vlassov, A. V.; Wang, Q.; Leake, D.; Ilves, H.; Gonzalez-Gonzalez, E.; Contag, C. H.; Johnston, B. H.; Kaspar, R. L. Stability Study of Unmodified siRNA and Relevance to Clinical Use. *Oligonucleotides* **2008**, *18* (4), 345–354.

(7) Sato, A.; Choi, S. W.; Hirai, M.; Yamayoshi, A.; Moriyarna, R.; Yamano, T.; Takagi, M.; Kano, A.; Shimamoto, A.; Maruyama, A. Polymer brush-stabilized polyplex for a siRNA carrier with long circulatory half-life. *J. Controlled Release* **2007**, *122* (3), 209–216.

(8) Jarve, A.; Muller, J.; Kim, I. H.; Rohr, K.; MacLean, C.; Fricker, G.; Massing, U.; Eberle, F.; Dalpke, A.; Fischer, R.; Trendelenburg, M. F.; Helm, M. Surveillance of siRNA integrity by FRET imaging. *Nucleic Acids Res.* **2007**, *35* (18), e124.

(9) Gao, S.; Dagnaes-Hansen, F.; Nielsen, E. J. B.; Wengel, J.; Besenbacher, F.; Howard, K. A.; Kjems, J. The effect of chemical modification and nanoparticle formulation on stability and biodistribution of siRNA in mice. *Mol. Ther.* **2009**, *17* (7), 1225–1233.

(10) Czauderna, F.; Fechtner, M.; Dames, S.; Aygun, H.; Klippel, A.; Pronk, G. J.; Giese, K.; Kaufmann, J. Structural variations and stabilising modifications of synthetic siRNAs in mammalian cells. *Nucleic Acids Res.* **2003**, *31* (11), 2705–2716.

(11) Kubo, T.; Zhelev, Z.; Ohba, H.; Bakalova, R. Modified 27-nt dsRNAs with dramatically enhanced stability in serum and long-term RNAi activity. *Oligonucleotides* **2007**, *17* (4), 445–464.

(12) Chiu, Y.-L.; Rana, T. M. siRNA function in RNAi: A chemical modification analysis. *RNA* **2003**, *9* (9), 1034–1048.

(13) Shukla, S.; Sumaria, C. S.; Pradeepkumar, P. I. Exploring chemical modifications for siRNA therapeutics: A structural and functional outlook. *ChemMedChem* **2010**, *5* (3), 328–349.

(14) Harborth, J.; Elbashir, S. M.; Vandenburgh, K.; Manninga, H.; Scaringe, S. A.; Weber, K.; Tuschl, T. Sequence, chemical, and structural variation of small interfering RNAs and short hairpin RNAs and the effect on mammalian gene silencing. *Antisense Nucleic Acid Drug Dev.* **2003**, *13* (2), 83–105.

(15) Lorenz, C.; Hadwiger, P.; John, M.; Vornlocher, H.-P.; Unverzagt, C. Steroid and lipid conjugates of siRNAs to enhance cellular uptake and gene silencing in liver cells. *Bioorg. Med. Chem. Lett.* **2004**, *14* (19), 4975–4977.

(16) Urban-Klein, B.; Werth, S.; Abuharbeid, S.; Czubayko, F.; Aigner, A. RNAi-mediated gene-targeting through systemic application of polyethylenimine (PEI)-complexed siRNA in vivo. *Gene Ther.* **2004**, *12* (5), 461–466.

(17) De Paula, D.; Bentley, M. V. L. B.; Mahato, R. I. Hydrophobization and bioconjugation for enhanced siRNA delivery and targeting. *RNA* **2007**, *13* (4), 431–456.

(18) Singh, N.; Agrawal, A.; Leung, A. K. L.; Sharp, P. A.; Bhatia, S. N. Effect of nanoparticle conjugation on gene silencing by RNA interference. *J. Am. Chem. Soc.* **2010**, *132* (24), 8241–8243.

(19) Morrissey, D. V.; Lockridge, J. A.; Shaw, L.; Blanchard, K.; Jensen, K.; Breen, W.; Hartsough, K.; Machemer, L.; Radka, S.; Jadhav, V.; Vaish, N.; Zinnen, S.; Vargeese, C.; Bowman, K.; Shaffer, C. S.; Jeffs, L. B.; Judge, A.; MacLachlan, I.; Polisky, B. Potent and persistent *in vivo* anti-HBV activity of chemically modified siRNAs. *Nat. Biotechnol.* **2005**, *23* (8), 1002–1007.

(20) Santel, A.; Aleku, M.; Keil, O.; Endruschat, J.; Esche, V.; Fisch, G.; Dames, S.; Loffler, K.; Fechtner, M.; Arnold, W.; Giese, K.; Klippel, A.; Kaufmann, J. A novel siRNA-lipoplex technology for RNA interference in the mouse vascular endothelium. *Gene Ther.* **2006**, *13* (16), 1222–1234.

(21) Zimmermann, T. S.; Lee, A. C. H.; Akinc, A.; Bramlage, B.; Bumcrot, D.; Fedoruk, M. N.; Harborth, J.; Heyes, J. A.; Jeffs, L. B.; John, M.; Judge, A. D.; Lam, K.; McClintock, K.; Nechev, L. V.; Palmer, L. R.; Racie, T.; Röhl, I.; Seiffert, S.; Shanmugam, S.; Sood, V.; Soutschek, J.; Toudjarska, I.; Wheat, A. J.; Yaworski, E.; Zedalis, W.; Koteliansky, V.; Manoharan, M.; Vornlocher, H.-P.; MacLachlan, I. RNAi-mediated gene silencing in non-human primates. *Nature* **2006**, *441* (7089), 111–114.

(22) Davis, M. E.; Zuckerman, J. E.; Choi, C. H. J.; Seligson, D.; Tolcher, A.; Alabi, C. A.; Yen, Y.; Heidel, J. D.; Ribas, A. Evidence of RNAi in humans from systemically administered siRNA via targeted nanoparticles. *Nature* **2010**, *464* (7291), 1067–1070.

(23) Huang, Y.-F.; Chang, H.-T.; Tan, W. Cancer Cell Targeting Using Multiple Aptamers Conjugated on Nanorods. *Anal. Chem.* **2008**, *80* (3), 567–572.

(24) Medley, C. D.; Smith, J. E.; Tang, Z.; Wu, Y.; Bamrungsap, S.; Tan, W. Gold Nanoparticle-Based Colorimetric Assay for the Direct Detection of Cancerous Cells. *Anal. Chem.* **2008**, *80* (4), 1067–1072.

(25) Rotello, V. Sniffing out cancer using "chemical nose" sensors. *Cell Cycle* **2009**, *8* (22), 3615–3616.

(26) You, C. C.; Miranda, O. R.; Gider, B.; Ghosh, P. S.; Kim, I. B.; Erdogan, B.; Krovi, S. A.; Bunz, U. H. F.; Rotello, V. M. Detection and identification of proteins using nanoparticle-fluorescent polymer 'chemical nose' sensors. *Nat. Nanotechnol.* **2007**, *2* (5), 318–323.

(27) Tkachenko, A. G.; Xie, H.; Coleman, D.; Glomm, W.; Ryan, J.; Anderson, M. F.; Franzen, S.; Feldheim, D. L. Multifunctional gold nanoparticle-peptide complexes for nuclear targeting. *J. Am. Chem. Soc.* **2003**, *125* (16), 4700–4701.

(28) Tkachenko, A. G.; Xie, H.; Liu, Y. L.; Coleman, D.; Ryan, J.; Glomm, W. R.; Shipton, M. K.; Franzen, S.; Feldheim, D. L. Cellular trajectories of peptide-modified gold particle complexes: Comparison of nuclear localization signals and peptide transduction domains. *Bioconjugate Chem.* **2004**, *15* (3), 482–490.

(29) Huang, C.-C.; Huang, Y.-F.; Cao, Z.; Tan, W.; Chang, H.-T. Aptamer-Modified Gold Nanoparticles for Colorimetric Determination of Platelet-Derived Growth Factors and Their Receptors. *Anal. Chem.* **2005**, *77* (17), 5735–5741.

(30) Agbasi-Porter, C.; Ryman-Rasmussen, J.; Franzen, S.; Feldheim, D. Transcription inhibition using oligonucleotide-modified gold nanoparticles. *Bioconjugate Chem.* **2006**, *17* (5), 1178–1183.

(31) Sandhu, K. K.; McIntosh, C. M.; Simard, J. M.; Smith, S. W.; Rotello, V. M. Gold nanoparticle-mediated Transfection of mammalian cells. *Bioconjugate Chem.* **2002**, *13* (1), 3–6.

(32) El-Sayed, I. H.; Huang, X. H.; El-Sayed, M. A. Surface plasmon resonance scattering and absorption of anti-EGFR antibody conjugated gold nanoparticles in cancer diagnostics: Applications in oral cancer. *Nano Lett.* **2005**, *5* (5), 829–834.

(33) El-Sayed, I. H.; Huang, X. H.; El-Sayed, M. A. Selective laser photo-thermal therapy of epithelial carcinoma using anti-EGFR antibody conjugated gold nanoparticles. *Cancer Lett.* **2006**, *239* (1), 129–135.

(34) Chithrani, B. D.; Chan, W. C. W. Elucidating the mechanism of cellular uptake and removal of protein-coated gold nanoparticles of different sizes and shapes. *Nano Lett.* **2007**, *7* (6), 1542–1550.

(35) Chithrani, B. D.; Ghazani, A. A.; Chan, W. C. W. Determining the size and shape dependence of gold nanoparticle uptake into mammalian cells *Nano Lett.* **2006**, *6* (4), 662–668.

(36) Mirkin, C. A.; Letsinger, R. L.; Mucic, R. C.; Storhoff, J. J. A DNA-based method for rationally assembling nanoparticles into macroscopic materials. *Nature* **1996**, *382* (6592), 607–609.

(37) Massich, M. D.; Giljohann, D. A.; Seferos, D. S.; Ludlow, L. E.; Horvath, C. M.; Mirkin, C. A. Regulating immune response using polyvalent nucleic acid-gold nanoparticle conjugates. *Mol. Pharmaceutics* **2009**, *6* (6), 1934–1940.

(38) Prigodich, A. E.; Lee, O. S.; Daniel, W. L.; Seferos, D. S.; Schatz, G. C.; Mirkin, C. A. Tailoring DNA structure to increase target hybridization kinetics on surfaces. *J. Am. Chem. Soc.* **2010**, *132* (31), 10638–10641.

(39) Seferos, D. S.; Giljohann, D. A.; Hill, H. D.; Prigodich, A. E.; Mirkin, C. A. Nano-flares: Probes for transfection and mRNA detection in living cells. *J. Am. Chem. Soc.* **2007**, *129* (50), 15477–15479.

(40) Seferos, D. S.; Prigodich, A. E.; Giljohann, D. A.; Patel, P. C.; Mirkin, C. A. Polyvalent DNA nanoparticle conjugates stabilize nucleic acids. *Nano Lett.* **2009**, *9* (1), 308–311.

(41) Elghanian, R.; Storhoff, J. J.; Mucic, R. C.; Letsinger, R. L.; Mirkin, C. A. Selective colorimetric detection of polynucleotides based on the distance-dependent optical properties of gold nanoparticles. *Science* **1997**, *277* (5329), 1078–1081.

(42) Taton, T. A.; Mirkin, C. A.; Letsinger, R. L. Scanometric DNA array detection with nanoparticle probes. *Science* **2000**, *289* (5485), 1757–1760.

(43) Nam, J. M.; Thaxton, C. S.; Mirkin, C. A. Nanoparticle-based bio-bar codes for the ultrasensitive detection of proteins. *Science* **2003**, *301* (5641), 1884–1886.

(44) Rosi, N. L.; Giljohann, D. A.; Thaxton, C. S.; Lytton-Jean, A. K. R.; Han, M. S.; Mirkin, C. A. Oligonucleotide-modified gold nanoparticles for intracellular gene regulation. *Science* **2006**, *312* (5776), 1027–1030.

(45) Giljohann, D. A.; Seferos, D. S.; Prigodich, A. E.; Patel, P. C.; Mirkin, C. A. Gene regulation with polyvalent siRNA-nanoparticle conjugates. *J. Am. Chem. Soc.* **2009**, *131* (6), 2072–2073.

(46) Giljohann, D. A.; Seferos, D. S.; Daniel, W. L.; Massich, M. D.; Patel, P. C.; Mirkin, C. A. Gold Nanoparticles for biology and medicine. *Angew. Chem., Int. Ed.* **2010**, *49* (19), 3280–3294.

(47) Lee, J. S.; Green, J. J.; Love, K. T.; Sunshine, J.; Langer, R.; Anderson, D. G. Gold, Poly(beta-amino ester) nanoparticles for small interfering RNA delivery. *Nano Lett.* **2009**, *9* (6), 2402–2406.

(48) Oishi, M.; Nakaogami, J.; Ishii, T.; Nagasaki, Y. Smart PEGylated gold nanoparticles for the cytoplasmic delivery of siRNA to induce enhanced gene silencing. *Chem. Lett.* **2006**, *35* (9), 1046–1047.

(49) Mitchell, G. P.; Mirkin, C. A.; Letsinger, R. L. Programmed Assembly of DNA Functionalized Quantum Dots. *J. Am. Chem. Soc.* **1999**, *121* (35), 8122–8123.

(50) Frens, G. Controlled nucleation for regulation of particle-size in monodisperse gold suspensions. *Nature (London), Phys. Sci.* **1973**, *241* (105), 20–22.

(51) Leuschner, P. J. F.; Martinez, J. *In vitro* analysis of microRNA processing using recombinant dicer and cytoplasmic extracts of HeLa cells. *Methods* **2007**, *43* (2), 105–109.

(52) Giljohann, D. A.; Seferos, D. S.; Patel, P. C.; Millstone, J. E.; Rosi, N. L.; Mirkin, C. A. Oligonucleotide loading determines cellular uptake of DNA-modified gold nanoparticles. *Nano Lett.* **2007**, *7* (12), 3818–3821.

(53) Rose, S. D.; Kim, D. H.; Amarzguioui, M.; Heidel, J. D.; Collingwood, M. A.; Davis, M. E.; Rossi, J. J.; Behlke, M. A. Functional polarity is introduced by dicer processing of short substrate RNAs. *Nucleic Acids Res.* **2005**, *33* (13), 4140–4156.

(54) Kim, D. H.; Behlke, M. A.; Rose, S. D.; Chang, M. S.; Choi, S.; Rossi, J. J. Synthetic dsRNA dicer substrates enhance RNAi potency and efficacy. *Nat. Biotechnol.* **2005**, *23* (2), 222–226.

(55) Vermeulen, A.; Behlen, L.; Reynolds, A.; Wolfson, A.; Marshall, W. S.; Karpilow, J.; Khvorova, A. The contributions of dsRNA structure to Dicer specificity and efficiency. *RNA* **2005**, *11* (5), 674–682.

(56) DiNitto, J. P.; Wang, L. Y.; Wu, J. C. Continuous fluorescence-based method for assessing Dicer cleavage efficiency reveals 3′ overhang nucleotide preference. *Biotechniques* **2010**, *48* (4), 303–309.

(57) Haupenthal, J.; Baehr, C.; Kiermayer, S.; Zeuzem, S.; Piiper, A. Inhibition of RNAse A family enzymes prevents degradation and loss of silencing activity of siRNAs in serum. *Biochem. Pharmacol.* **2006**, *71* (5), 702–710.

(58) Amarzguioui, M.; Holen, T.; Babaie, E.; Prydz, H. Tolerance for mutations and chemical modifications in a siRNA. *Nucleic Acids Res.* **2003**, *31* (2), 589–595.

(59) Braasch, D. A.; Jensen, S.; Liu, Y.; Kaur, K.; Arar, K.; White, M. A.; Corey, D. R. RNA interference in mammalian cells by chemically-modified RNA. *Biochemistry* **2003**, *42* (26), 7967–7975.

(60) Collingwood, M. A.; Rose, S. D.; Huang, L. Y.; Hillier, C.; Amarzguioui, M.; Wiiger, M. T.; Soifer, H. S.; Rossi, J. J.; Behlke, M. A. Chemical modification patterns compatible with high potency Dicer-substrate small interfering RNAs. *Oligonucleotides* **2008**, *18* (2), 187–199.

(61) Elmen, J.; Thonberg, H.; Ljungberg, K.; Frieden, M.; Westergaard, M.; Xu, Y. H.; Wahren, B.; Liang, Z. C.; Urum, H.; Koch, T.; Wahlestedt, C. Locked nucleic acid (LNA) mediated improvements in siRNA stability and functionality. *Nucleic Acids Res.* **2005**, *33* (1), 439–447.

(62) Kubo, T.; Zhelev, Z.; Ohba, H.; Bakalova, R. Chemically modified symmetric and asymmetric duplex RNAs: An enhanced stability to nuclease degradation and gene silencing effect. *Biochem. Biophys. Res. Commun.* **2008**, *365* (1), 54–61.

(63) Manoharan, M. RNA interference and chemically modified small interfering RNAs. *Curr. Opin. Chem. Biol.* **2004**, *8* (6), 570–579.

(64) Mook, O. R.; Baas, F.; de Wissel, M. B.; Fluiter, K. Evaluation of locked nucleic acid-modified small interfering RNA *in vitro* and *in vivo*. *Mol. Cancer Ther.* **2007**, *6* (3), 833–843.

(65) Raemdonck, K.; Remaut, K.; Lucas, B.; Sanders, N. N.; Demeester, J.; De Smedt, S. C. *In situ* analysis of single-stranded and duplex siRNA integrity in living cells. *Biochemistry* **2006**, *45* (35), 10614–10623.

(66) Choung, S.; Kim, Y. J.; Kim, S.; Park, H. O.; Choi, Y. C. Chemical modification of siRNAs to improve serum stability without loss of efficacy. *Biochem. Biophys. Res. Commun.* **2006**, *342* (3), 919–927.

(67) Lan, T.; Putta, M. R.; Wang, D. Q.; Dai, M. R.; Yu, D.; Kandimalla, E. R.; Agrawal, S. Synthetic oligoribonucleotides-containing secondary structures act as agonists of Toll-like receptors 7 and 8. *Biochem. Biophys. Res. Commun.* **2009**, *386* (3), 443–448.

(68) Glud, S. Z.; Bramsen, J. B.; Dagnaes-Hansen, F.; Wengel, J.; Howard, K. A.; Nyengaard, J. R.; Kjems, J. Naked siLNA-mediated gene silencing of lung bronchoepithelium eGFP expression after intravenous administration. *Oligonucleotides* **2009**, *19* (2), 163–168.

(69) Turner, J. J.; Jones, S. W.; Moschos, S. A.; Lindsay, M. A.; Gait, M. J. MALDI-TOF mass spectral analysis of siRNA degradation in serum confirms an RNAse A-like activity. *Mol. BioSyst.* **2007**, *3* (1), 43–50.

(70) Mathews, D. H.; Sabina, J.; Zuker, M.; Turner, D. H. Expanded sequence dependence of thermodynamic parameters improves prediction of RNA secondary structure. *J. Mol. Biol.* **1999**, *288* (5), 911–940.

(71) Patel, P. C.; Giljohann, D. A.; Daniel, W. L.; Zheng, D.; Prigodich, A. E.; Mirkin, C. A. Scavenger Receptors Mediate Cellular Uptake of Polyvalent Oligonucleotide-Functionalized Gold Nanoparticles. *Bioconjugate Chem.* **2010**, *21* (12), 2250–2256.